Patterns of Proliferation and Apoptosis during Murine Hair Follicle Morphogenesis

Markus Magerl,* Desmond J. Tobin,† Sven Müller-Röver,*‡§ Evelin Hagen,* Gerd Lindner,* Ian A. McKay,‡ and Ralf Paus*§

*Department of Dermatology, Charité, Humboldt-University, Berlin, Germany; †Department of Biomedical Sciences, University of Bradford, Bradford, West Yorkshire, U.K.; ‡Centre for Cutaneous Research, Queen Mary and Westfield College, University of London, U.K.; §Department of Dermatology, University Hospital Eppendorf, University Hamburg, Hamburg, Germany

In this study, we have correlated cutaneous apoptosis and proliferation in neonatal mice during hair follicle morphogenesis. We have applied a novel triple-staining technique that uses Ki67 immunoreactivity as a marker of proliferation as well as TUNEL and Hoechst 33342 staining as apoptosis markers. We have also assessed the immunoreactivity of interleukin-1β-converting enzyme, caspase 1, a key enzyme in the execution of apoptosis, and of P-cadherin, which has been suggested as a key adhesion receptor in segregating proliferating keratinocytes. The TUNEL data were systematically compared with high resolution light microscopy and transmission electron microscopy data. Virtually all keratinocytes of the developing hair bud were strongly Ki67$^+$, suggesting that the hair bud is not an epidermal invagination but primarily the product of localized keratinocyte proliferation. As hair follicle development advanced, three distinct foci of proliferation became apparent: the distal outer root sheath around the hair canal, the mid outer root sheath, and the proximal hair matrix. Of these proliferating hair follicle keratinocytes only defined subsets expressed P-cadherin. TUNEL$^+$ cells in the hair follicle were not found before stage 5 of murine hair follicle morphogenesis. During the early stages of hair follicle development, interleukin-1β-converting enzyme immunoreactivity was present on all keratinocytes, but virtually disappeared from the proximal hair follicle epithelium later on. High resolution light microscopy/transmission electron microscopy revealed scattered and clustered apoptotic keratinocytes in all epithelial hair follicle compartments throughout hair follicle development, including its earliest stages. This highlights striking differences in the demarcation of apoptotic hair follicle keratinocytes between the TUNEL technique and high resolution light microscopy/transmission electron microscopy and suggests a role for apoptosis in sculpting the hair follicle even during early hair follicle development. ***Key words: apoptosis/ICE/Ki67/P-cadherin/transmission electron microscopy/TUNEL. J Invest Dermatol 116:947–955, 2001***

Hair follicle (HF) pattern formation is a complex process of organogenesis that is tightly regulated by a well-balanced interplay of cell proliferation, polarization, differentiation, and programmed cell death (Glücksmann, 1951; Saunders, 1966; Paus *et al*, 1993). Previously, Polakowska *et al* (1994) reported prominent apoptosis in the epithelium of the developing human HF. In that study, however, the relative contribution of apoptosis to HF morphogenesis, and its coordination with epithelial cell proliferation, adhesion molecule expression, and caspase expression were not systematically assessed. Thus, no comprehensive apoptosis study is yet available on murine hair follicle development, a very instructive research model for general studies on morphogenesis (Gat *et al*, 1998; Oro and Scott, 1998; Philpott and Paus, 1998; St Jacques *et al*, 1998; Botchkarev *et al*, 1999). One key question in hair biology is the long-standing controversy whether HF morphogenesis is primarily a cell-migration-driven invagination of the epidermis or whether HF development rather reflects a highly restricted and stringently regulated burst of keratinocyte (KC) proliferation and segregation, which leads to hair bud formation (Danneel, 1931; Fleischhauer, 1953; Pinkus, 1958; Müller *et al*, 1991; Paus *et al*, 1999). Therefore, this study aimed at characterizing and covisualizing the patterns of proliferation and apoptosis during murine HF morphogenesis using the C57BL/6J mouse model (Paus *et al*, 1999). Apoptotic (i.e., TUNEL$^+$) and proliferating (i.e., Ki67$^+$) cells were covisualized by employing a novel immunofluorescent triple-staining protocol that utilizes the DNA dye Hoechst 33342 as a nuclear counterstain. Furthermore, we have studied the coexpression patterns of Ki67 with P-cadherin, which has been suggested to be a key adhesion receptor for the segregation of proliferating KC in the epidermis and in the HF (Hirai *et al*, 1989; Shimoyama *et al*, 1989). In addition, the codistribution of TUNEL$^+$ cells with interleukin-1β-converting enzyme (caspase-1, ICE) immunoreactivity (IR) was assessed in order to correlate apoptosis with the follicular distribution of this key caspase in the death execution machinery (Darmon and

Manuscript received February 16, 1999; revised December 22, 2000; accepted for publication March 12, 2001.

Reprint requests to: Dr. Ralf Paus, Hautklinik, Universitäts-Krankhaus Eppendorf, Universität Hamburg, Martinistr. 52, D-20246 Hamburg, Germany. Email: paus@uke.uni-hamburg.de

Abbreviations: DP dermal papilla; HF, hair follicle; HM, hair matrix; HRLM, high resolution light microscopy; ICE, interleukin-1β-converting enzyme, caspase 1; IR, immunoreactivity; KC, keratinocyte; TUNEL, TdT-mediated dUTP-digoxigenin nick end labeling.

Bleackley, 1996; Zhivotovsky *et al*, 1996; Trump *et al*, 1997; Allen *et al*, 1998).

MATERIALS AND METHODS

Animals and tissue collection C57BL/6 mice of both sexes (Charles River, Sulzfeld, Germany) were housed in community cages under 12 h light periods, and were fed water and mouse chow *ad libitum*. All hair cycle stages of neonatal HF morphogenesis (stages 0–8) were studied as described previously (Paus *et al*, 1999).

Immunohistochemistry The TUNEL technique (TdT-mediated dUTP-digoxigenin nick end labeling, ApopTag, Oncor) was combined with the nuclear stain Hoechst 33342 and an antibody against ICE or Ki67 as previously described (Lindner *et al*, 1997; Botchkarev *et al*, 1998). Eight micron cryostat sections of C57BL/6 back skin were freshly prepared and fixed in formalin (10%) for 10 min at room temperature and postfixed in ethanol/acetic acid (2:1) for 5 min at –20°C. The sections were then covered with equibrilation buffer for 5 min at room temperature, followed by incubation with terminal deoxynucleotidyl transferase (TdT) solution for 1 h at 37°C. This reaction was terminated with stop/wash buffer for 30 min at 37°C. After blocking with normal goat serum [10% in phosphate-buffered saline (PBS), 20 min), the sections were incubated with the primary antibody (ICE or Ki67, 1:100 in PBS, overnight, 4°C). Digoxigenin-dUTP labeled DNA compounds were detected by antidigoxigenin fluorescein isothiocyanate conjugated F(ab)2 fragments (30 min at room temperature). Thereafter, the tissue was covered with the secondary antibody solution (goat anti-rabbit rhodamine, 1:200 in PBS, 30 min, room temperature). Tissue sections were counterstained for 45 min at room temperature with Hoechst 33342 dye (10 μg per ml in PBS). Each staining phase was interspersed by a washing step (three times) in PBS. The antibody used for ICE (Santa Cruz Biotechnology, Santa Cruz, CA) detects the p10 subunit of the murine ICE-heterodimer and recognizes both the inactive and the active form of ICE (Bhat *et al*, 1996; Shimizu *et al*, 1996). The antibody employed to detect the proliferation-associated antigen Ki67 (Dianova, Hamburg, Germany) is a monoclonal antibody to a 345–395 kDa protein complex (Gerdes *et al*, 1991) expressed primarily during the S, G_2, and M phases of the cell cycle (Sawhney and Hall, 1992; Schwarting, 1993; Gerlach *et al*, 1997).

Hoechst 33342 (2′-[4-ethoxyphenyl]-5-[4-methyl-1-piperazinyl]-2,5′-bi-1h-benzimidazole; Sigma Chemical, Diesenhofen, Germany) is a nonintercalating (Sailer *et al*, 1997) DNA-reactive fluorochrome with preferential binding to A–T regions (Crissman and Steinkamp, 1993). It serves as both a nuclear counterstain and a morphologic indicator of apoptotic cells (Hardin *et al*, 1992).

For the P-cadherin/Ki67/Hoechst 33342 triple staining, we used a slightly modified version of the protocol established for TUNEL/Ki67/Hoechst 33342 triple staining (Lindner *et al*, 1997). The rat monoclonal antimouse P-cadherin antibody PCD-1 (Nose and Takeichi, 1986) was applied in a dilution of 1:50.

The IR patterns were evaluated with a fluorescence microscope (Zeiss, Oberkochen, Germany), using the appropriate filters. Photomicrographs were generated with the help of a digital image analysis system (ISIS, Metasystems, Belmont, MA).

High resolution light microscopy (HRLM) and transmission electron microscopy (TEM) Representative tissue samples were obtained from two sites on the backs of 15 mice (three mice each at 0, 1, 3, 5 and 8 d *post partum*) for a total of 60 blocks from 30 mice. The tissues were fixed in Karnovsky's fixative (Karnovsky, 1965), postfixed in 2% osmium tetroxide, uranyl acetate, and phenylenediamine, and embedded in resin as previously described (Tobin *et al*, 1990; 1991). Semi-thin and ultra-thin sections were cut with a Reichart–Jung microtome; the former were stained with the metachromatic stain, toluidine blue/borax, examined by oil-immersion light microscopy, and photographed (Leitz, Wetzlar, Germany). The latter were stained with uranyl acetate and lead citrate and examined and photographed using a Jeol 100CX electron microscope (Jeol, Tokyo, Japan). Sixty HF at each time point were examined by light microscopy from each mouse (total of 300 HF) and 30 HF from each by TEM (total of 150 HF).

RESULTS AND DISCUSSION

This study provides strong evidence that the formation of the new HF is based on a tightly regulated and strictly coordinated interplay of apoptosis and cell proliferation, which occurs in a focal rather than a random pattern. Cell death, remarkably, was a significant feature of HF morphogenesis even in its earliest stages.

Figure 1. Distribution of TUNEL$^+$ and ICE$^+$ or Ki67$^+$ cells during murine HF morphogenesis. TUNEL staining has been used as an apoptosis marker, Hoechst 33342 has been used as a nuclear counterstain and additional apoptosis marker, and Ki67 has been used as a marker of proliferation; ICE is a key enzyme of apoptosis execution, and P-cadherin has been suggested as a key adhesion receptor for proliferating KC compartments. (*a–j*) A triple stain with TUNEL (green), Ki67 (pink), and Hoechst 33342 (blue). (*k–v*) A triple stain with TUNEL (green), ICE (red), and Hoechst 33342 (blue). (*w–z*) A triple stain with P-cadherin (green), Ki67 (pink), and Hoechst 33342 (blue). *Upper left-hand corner*: stage of HF morphogenesis. *Scale bar*: 50 μm. (*a*) Stage 0, TUNEL–Ki67–Hoechst 33342 triple stain. Scattered Ki67$^+$ cells were found in the basal layer (b) of the epidermis (e) of murine skin harvested at the day of birth. *Arrowhead*: TUNEL$^+$ cell. (*b*) Stage 1, TUNEL–Ki67–Hoechst 33342 triple stain. Selected cells in the basal layer are Ki67$^+$ (*dotted line*). (*c*) Stage 2, TUNEL–Ki67–Hoechst 33342 triple stain. Proliferating, strongly Ki67$^+$ hair germ (hg). *Arrowhead*: TUNEL$^+$ cell. (*d*) Stage 3, TUNEL–Ki67–Hoechst 33342 triple stain. Ki67-negative DP fibroblasts; hair bud KC remain Ki67$^+$, particularly above the DP. (*e*) Stage 4, TUNEL–Ki67–Hoechst 33342 triple stain. The Ki67 IR gets restricted to the HM (bulb), the developing ORS, and the epidermis (e). The DP and the IRS remain Ki67 negative. (*f*) Stage 5, TUNEL–Ki67–Hoechst 33342 triple stain. Ki67$^+$ HM around DP and ORS. *Arrowhead*: TUNEL$^+$ KC. (*g*) Stage 6, TUNEL–Ki67–Hoechst 33342 triple stain. Ki67$^+$ HM (b); distal ORS; Ki67 negative proximal ORS. *Arrowhead*: TUNEL$^+$ cell. (*h*) Stage 7, TUNEL–Ki67–Hoechst 33342 triple stain. Ki67$^+$ distal ORS (infundibular region). (*i, j*) Stage 8, TUNEL–Ki67–Hoechst 33342 triple stain. Strong Ki67 IR on the KC of the HM, the middle, and the very distal ORS around the hair canal (hc) and weaker staining of epidermal KC. The DP and the IRS remain Ki67 negative. (*k*) Stage 0, TUNEL–ICE–Hoechst 33342 triple stain. Strong ICE IR on KC of strata basale, spinosum, and granulosum. *Arrowhead*: TUNEL$^+$ cell. (*l*) Stage 1, TUNEL–ICE–Hoechst 33342 triple stain. All epidermal KC display strong ICE IR. *Arrowhead*: TUNEL$^+$ cell. (*m*) Stage 2, TUNEL–ICE–Hoechst 33342 triple stain. Proliferating, strongly ICE$^+$ KC of the developing hair peg (hp). *Arrowhead*: TUNEL$^+$ cell. (*n*) Stage 3, TUNEL–ICE–Hoechst 33342 triple stain. DP fibroblasts are ICE negative, whereas the KC of epidermis (e) and hair peg (hp) are ICE$^+$. (*o*) Stage 4, TUNEL–ICE–Hoechst 33342 triple stain. The newly generated IRS cells express strong ICE IR, whereas KC of the proximal hair bulb, in particular the KC of the developing HM, display virtually no ICE IR. (*p*) Stage 5, TUNEL–ICE–Hoechst 33342 triple stain. The emerging IRS and the ORS showed strong ICE IR. Hair bulb KC and DP fibroblasts remained ICE negative. *Arrowhead*: TUNEL$^+$ KC. (*q*) Stage 6, TUNEL–ICE–Hoechst 33342 triple stain. The emerging sebocytes show strong ICE IR as well as the IRS, and the bulge and isthmus region of the ORS. *Arrowhead*: TUNEL$^+$ KC. (*r*) Stage 7, TUNEL–ICE–Hoechst 33342 triple stain. Similar to previous developmental stages KC of the distal ORS as well as epidermal KC show strong ICE IR. Compared to the epidermis, the IRS displays substantially weaker ICE IR. *Arrowheads*: TUNEL$^+$ KC. (*s–v*) Stage 8, TUNEL–ICE–Hoechst 33342 triple stain. Micrographs (*t*), (*u*), and (*v*) are sequential horizontal sections prepared from different levels of the HF epithelium: (*t*) hair canal; (*u*) distal HF; (*v*) the central HF. ICE IR becomes virtually absent in the distal and mid IRS and remains strong in the mid ORS as well as in the distal ORS at the level of the hair canal (hc) region. *Arrowheads*: TUNEL$^+$ KC. (*w*) Stage 2, Ki67–P-cadherin–Hoechst 33342 triple stain. Commonly colocalized Ki67 and P-cadherin IR in the same cells of the hair germ (hg). No expression on DP fibroblasts. (*x*), (*y*) Stages 4 and 6, Ki67–P-cadherin–Hoechst 33342 triple stain. The coexpression of Ki67 and P-cadherin became restricted to the innermost portion of the HM around the DP and the mid ORS. Isolated P-cadherin in the precortical matrix (*arrows*) and in the sebaceous gland (sg) as well as isolated Ki67 IR on the KC of the outermost portion of the HM. (*z*) Stage 8, Ki67–P-cadherin–Hoechst 33342 triple stain. Strong coexpression of Ki67 and P-cadherin on the innermost portion of the hair matrix (hm) around the DP. Isolated P-cadherin in the precortical matrix (*arrows*) and isolated Ki67 IR on the KC of the outermost portion of the HM. b, basal layer; dp, dermal papilla; e, epidermis; hf, hair follicle; hm, hair matrix; hp, hair peg; irs, inner root sheath; kc, keratinocyte; ors, outer root sheath.

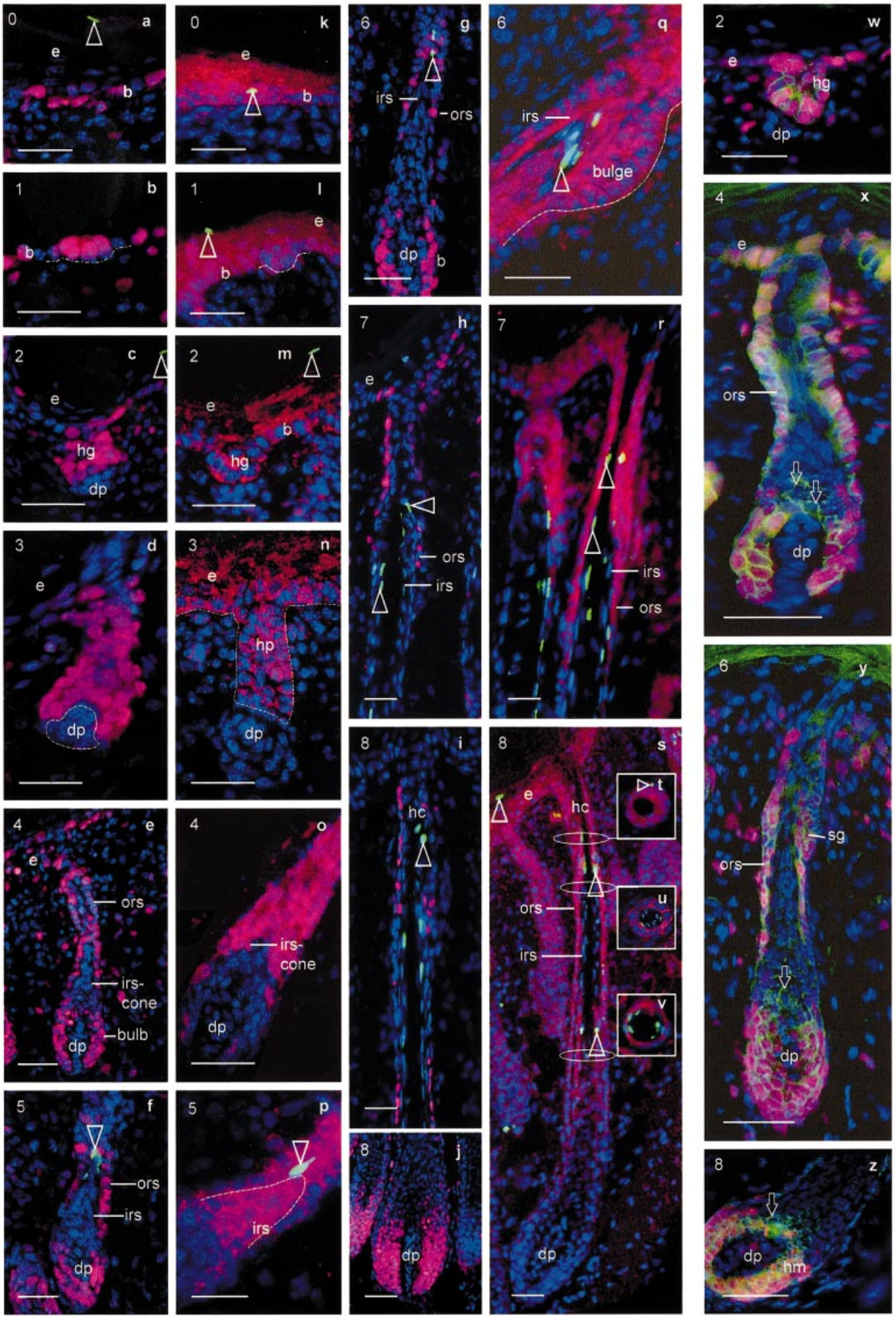
0 a
e
b
0 k
e
b
6 g
irs
ors
dp
b
6 q
irs
bulge
2 w
e
hg
dp
1 b
b
1 l
e
b
4 x
e
ors
dp
2 c
e
hg
dp
2 m
e
b
hg
7 h
e
ors
irs
7 r
irs
ors
3 d
e
dp
3 n
e
hp
dp
6 y
sg
ors
dp
4 e
e
ors
irs-
cone
bulb
dp
4 o
irs-
cone
dp
8 i
hc
8 s
e
hc
t
ors
u
irs
v
dp
5 f
ors
irs
dp
5 p
irs
8 j
dp
8 z
dp
hm

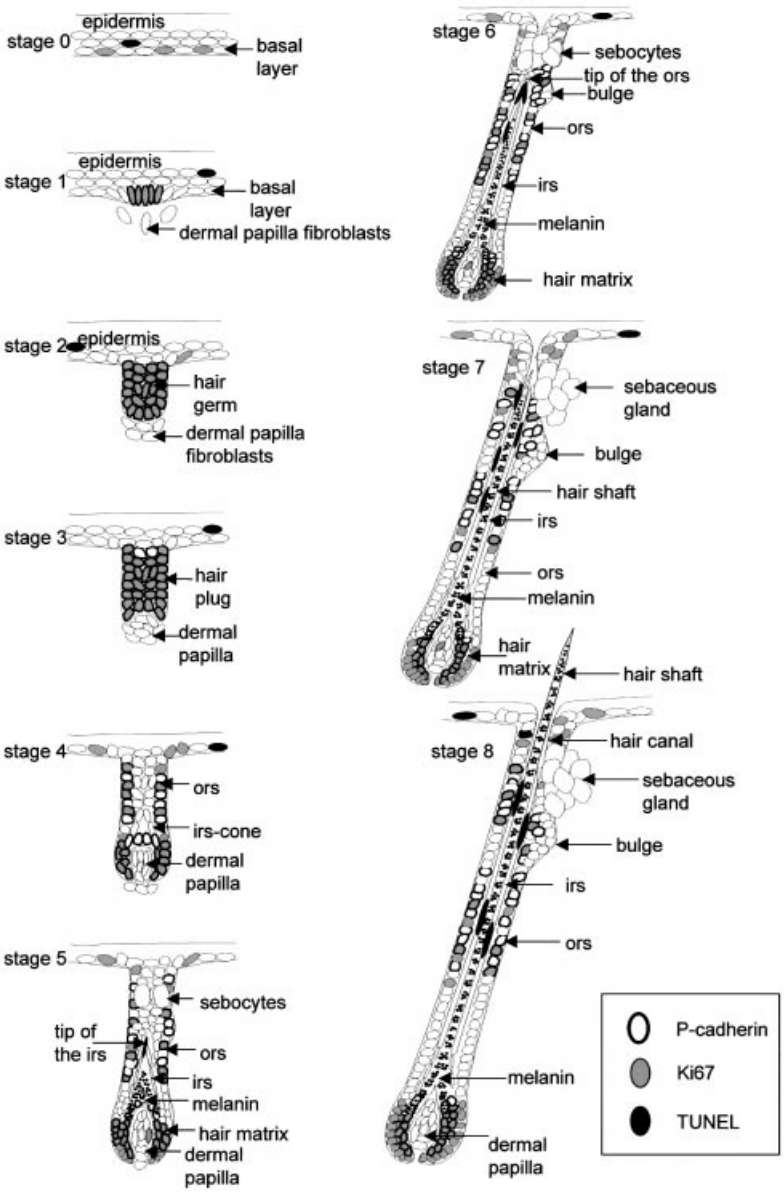

Figure 2. Distribution of TUNEL$^+$, Ki67$^+$, and P-cadherin$^+$ cells during murine HF morphogenesis. Schematic representation of TUNEL labeling (black) and Ki67 (gray) and P-cadherin (black membrane) IR during all stages of HF development. irs, inner root sheath; ors, outer root sheath.

Cell proliferation during HF morphogenesis Ki67$^+$ cells were rare in the undifferentiated basal layer of the epidermis (**Fig 1*a***). In contrast, virtually all HF KC in morphogenesis stages 1 and 2 were strongly and homogeneously Ki67$^+$ (**Fig 1*b***, ***c***), indicating that they had entered into the cell cycle (Sawhney and Hall, 1992; Schwarting, 1993; Gerlach *et al*, 1997). This homogeneous Ki67 IR of early hair buds (**Figs 1*b–d***, **2**) provides very suggestive evidence for the old concept that hair bud formation is the consequence of massive KC proliferation in a well-defined region of the epidermis, rather than resulting primarily from epithelial cell migration from the epidermis – so-called epidermal ''invagination'' (Danneel, 1931; Fleischhauer, 1953; Pinkus, 1958).

A more heterogeneous distribution of Ki67$^+$ cells was a feature of stage 3 HF (**Fig 1*d***), which became increasingly more restricted in maturing HFs to three distinct foci of proliferation (**Figs 1*e–j***, **2**): the distal outer root sheath (ORS) around the hair canal (**Fig 1*i***), the mid ORS (**Figs 1*i***, **4*l***), and the proximal hair matrix (HM) (**Fig 1*j***). The number of Ki67$^+$ cells in the proximal ORS declined during stage 5 (**Fig 1*f***). When the HF reached its largest extension in stage 8, the hair bulb KC showed maximal Ki67 IR (**Fig 1*j***), particularly below Auber's line (Bullough and Laurence, 1958; Ramirez *et al*, 1997). Whereas TRITC labeling did not reveal any Ki67 IR on dermal papilla (DP) fibroblasts at any time during neonatal skin and HF development, the more sensitive avidin–biotin complex labeling technique (Müller-Röver *et al*, 1998) revealed Ki67$^+$ DP fibroblasts located in the pre-DP and DP throughout all stages of HF morphogenesis (**Fig 3*b***, ***d***, ***f***, ***h***, ***j***). Ki67$^+$ fibroblasts were also located in the connective tissue sheath (CTS) during stages 3 and 4 (**Fig 3*f***, ***h***). These findings were confirmed by HRLM (**Fig 3*a***, ***c***, ***e***, ***g***, ***i***).

P-cadherin expression during HF morphogenesis P-cadherin expression has been suggested by some as a useful marker for discriminating proliferating and nonproliferating epidermal and follicular KC (Hirai *et al*, 1989; Shimoyama *et al*, 1989; Fujita *et al*, 1992; Müller-Röver *et al*, 1999). Ki67 and P-cadherin IR were very commonly co-localized in the same cells during HF morphogenesis stages 0–2, where homogeneous staining occurred in all follicular KC (**Fig 1*w***). This co-expression pattern became restricted to the innermost portion of the HM, however, and to the mid ORS during stages 3–6 (**Fig 1*x***, ***y***). In contrast to

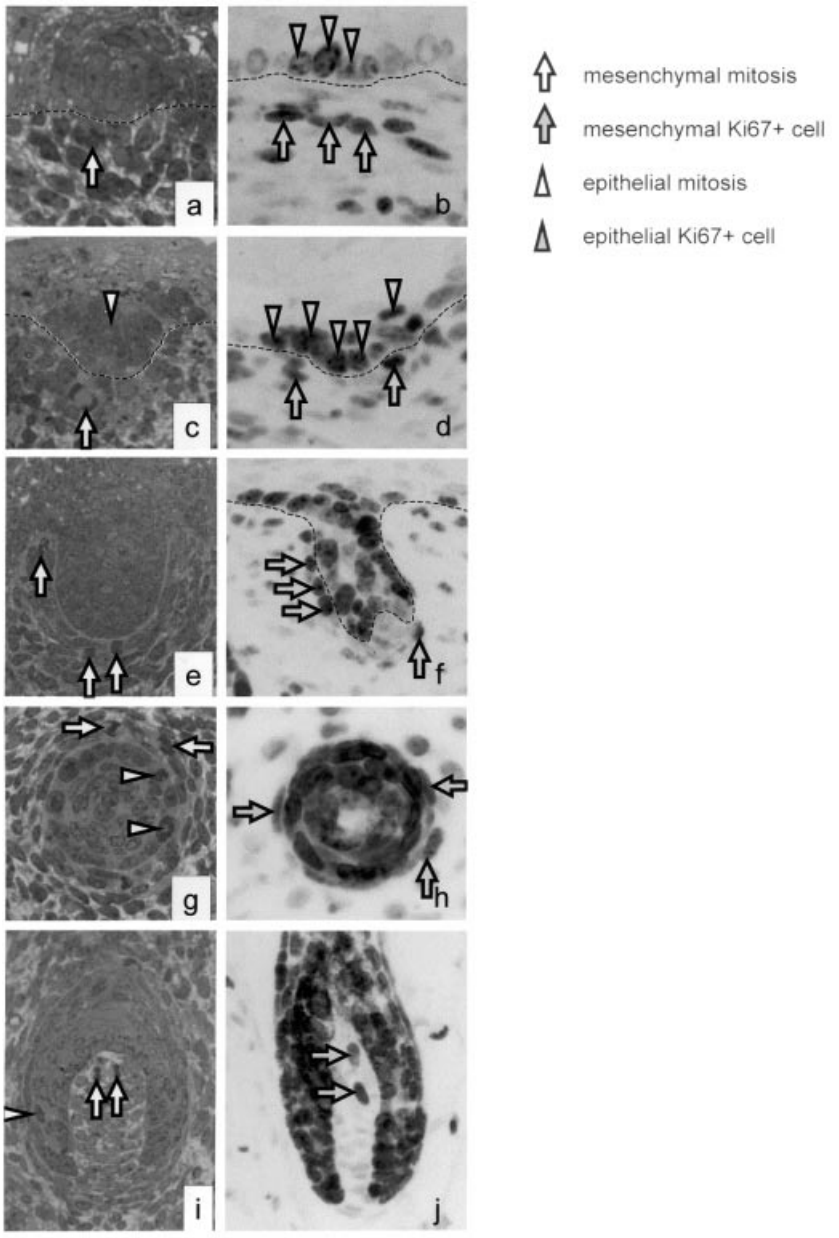

Figure 3. Proliferation of mesenchymal cells during HF morphogenesis. HRLM analysis revealed mitotic fibroblasts in the pre-DP [(*a*) stage 1, (*c*) stage 2] and DP [(*e*) stage 3, (*i*) stage 4–5]. Similarly, $Ki67^+$ fibroblasts were located in the pre-DP [(*b*) stage 1, (*d*) stage 2)] and DP [(*f*) stage 3, (*j*) stage 5]. Proliferating fibroblasts were also located in the CTS [(*e*, *f*) stage 3, (*g*, *h*) stage 4]. All stages of hair follicle morphogenesis according to Paus *et al* (1999). Note that TRITC labeling did not reveal any $Ki67^+$ fibroblasts in the DP, whereas the avidin–biotin complex labeling technique applied here is more sensitive (Müller-Röver *et al*, 1998).

Figure 4. HRLM and TEM analysis of proliferation and apoptosis during hair follicle morphogenesis. Figures display longitudinal sections of developing hair follicles. (*a*) HRLM. Stage 1 HF. Note the presence of three apoptotic cells (*arrowheads*) located above columnar basal KC. (*b*) HRLM. Stage 2 HF. Note the presence of a single apoptotic cell (*arrowhead*) in the developing HF with classic apoptotic features including (i) rounding up of the cell and shrinkage from surrounding healthy cells, (ii) the rounding up and condensation of the nucleus, and (iii) the hyperchromatism of the cytoplasm. This cell has yet to be engulfed by surrounding cells. e, epidermis; d, dermis; v, vessel. (*c*) TEM. Stage 2 HF. Note KC mitosis in the developing HF (*encircled area*). (*d*) HRLM. Stage 3 HF (*dotted line*). Note the presence of three apoptotic cells (*arrowheads*) in the matrix just above the DP in close proximity to mitotic cell (*encircled region*). (*e*) HRLM. Note the formation of the IRS. Some of these differentiating IRS cells have a passing resemblance to pyknotic cells (*arrowheads*). Compare them with $TUNEL^+$ cells in **Fig 1**(***f***, ***g***) and **1**(***p***, ***q***). (*f*) TEM. Stage 5 HF. At the tip of the developing inner root sheath (irs) note nuclear remnants in the keratinizing IRS. Compare them with $TUNEL^+$ cells in **Fig 1**(***f***, ***g***) and **1**(***p***, ***q***). ors, outer root sheath. (*g*) HRLM. Stage 6 HF. Note the presence of three apoptotic cells (*arrowheads*) in the precortex of the hair bulb. Note also the upper apoptotic cell with classic apoptotic features including contraction of the cell and nuclear condensation. dp, dermal papilla. (*h*) TEM. Stage 6 HF. Tip of the developing hair cone. Note presence of three apoptotic KC (*arrowheads*) adjacent to the outer root sheath (ors). (*i*) TEM. Apoptotic KC (*arrowheads*) of **Fig 1**(***h***) in higher magnification. Note classic apoptotic features: contraction of the cell and nuclear condensation (left), vacuolization (right). Note also the retention of organelle integrity (right, at the bottom). (*j*) TEM. Stage 6 HF. Tip of hair cone passing by the sebocytes of developing sebaceous gland. *Arrowhead*: apoptotic cell; ors, outer root sheath. (*k*) TEM. Stage 6 HF. Higher magnification of the apoptotic cell (*arrowhead*) in **Fig 1**(***j***). Note cell shrinkage and vacuolization. (*l*) TEM. Stages 6–7 HF. Mitotic KC in the middle outer root sheath (ors). (*m*) TEM. Stage 7 HF. Hair cone including apoptotic KC (*arrowheads*). Note nuclear emargination, cell body shrinkage, and cytoplasmic vacuolization. Ors, outer root sheath. (*n*) TEM. Stage 8 HF. Note the presence of degenerating cell in the middle outer root sheath (ors) close to the inner root sheath (irs). There appears to be a breakdown of the nuclear material into condensed spherical structures (*arrowhead*) without typical apoptosis-associated changes in cell shape. he, Henle's layer; hu, Huxley's layer; irs, inner root sheath; ors, outer root sheath. (*o*) TEM. Longitudinal section of distal HF at level of the sebaceous gland. Note phagocytosis of apoptotic bodies (*arrowhead*) in the outer root sheath (ors). The apoptotic body consists of a highly condensed and electron dense nuclear fraction in addition to condensed cytoplasm. Note also copious amounts of glycogen in ORS KC. Lobules of the sebaceous gland (sg) appear in the upper part.

human skin development (Fujita *et al*, 1992), we show here that KC in the outermost portion of the murine HM display isolated Ki67 IR but no P-cadherin IR (**Figs 1*x*–*z*, 2**), whereas KC in the precortical murine HM display isolated P-cadherin IR and no Ki67 IR (**Figs 1*x*–*z*, 2**). This suggests that follicular P-cadherin expression is much less tightly coupled to the proliferative epithelial cell compartment than previously proposed (Hirai *et al*, 1989; Shimoyama *et al*, 1989).

Cell death during HF morphogenesis Throughout HF morphogenesis, scattered TUNEL$^+$ cells were observed in the epidermis, most commonly in the stratum granulosum (**Fig 1*a*, *c*, *k*, *l*, *m*, *s***). In contrast, intrafollicular TUNEL$^+$ cells were never observed during the first stages of HF development (stages 1–4) (**Fig 1*a*–*e*, *k*–*o***) and appeared first during stage 5. Interestingly, they were frequently seen just in and above the newly generated inner root sheath (IRS) (**Fig 1*f*, *p***). During stage 6, several strongly TUNEL$^+$ cells with an elongated, flattened appearance became visible in the IRS at the level of the tip of the emerging hair shaft (**Fig 1*g*, *q***). Additional TUNEL$^+$ cells appeared in the mid IRS as well as in the distal and infundibular ORS during stages 7 and 8 (**Fig 1*h*, *i*, *r*, *s***).

Clustering of TUNEL$^+$ cells, as is characteristic of hair follicle regression (catagen) (Lindner *et al*, 1997), occurred only late in HF development. During stages 7 and 8 of HF morphogenesis, TUNEL$^+$ cells were concentrated within three distinct apoptosis "hot spots", namely the distal and mid IRS and the infundibular ORS, similar to human HF development (Polakowska *et al*, 1994).

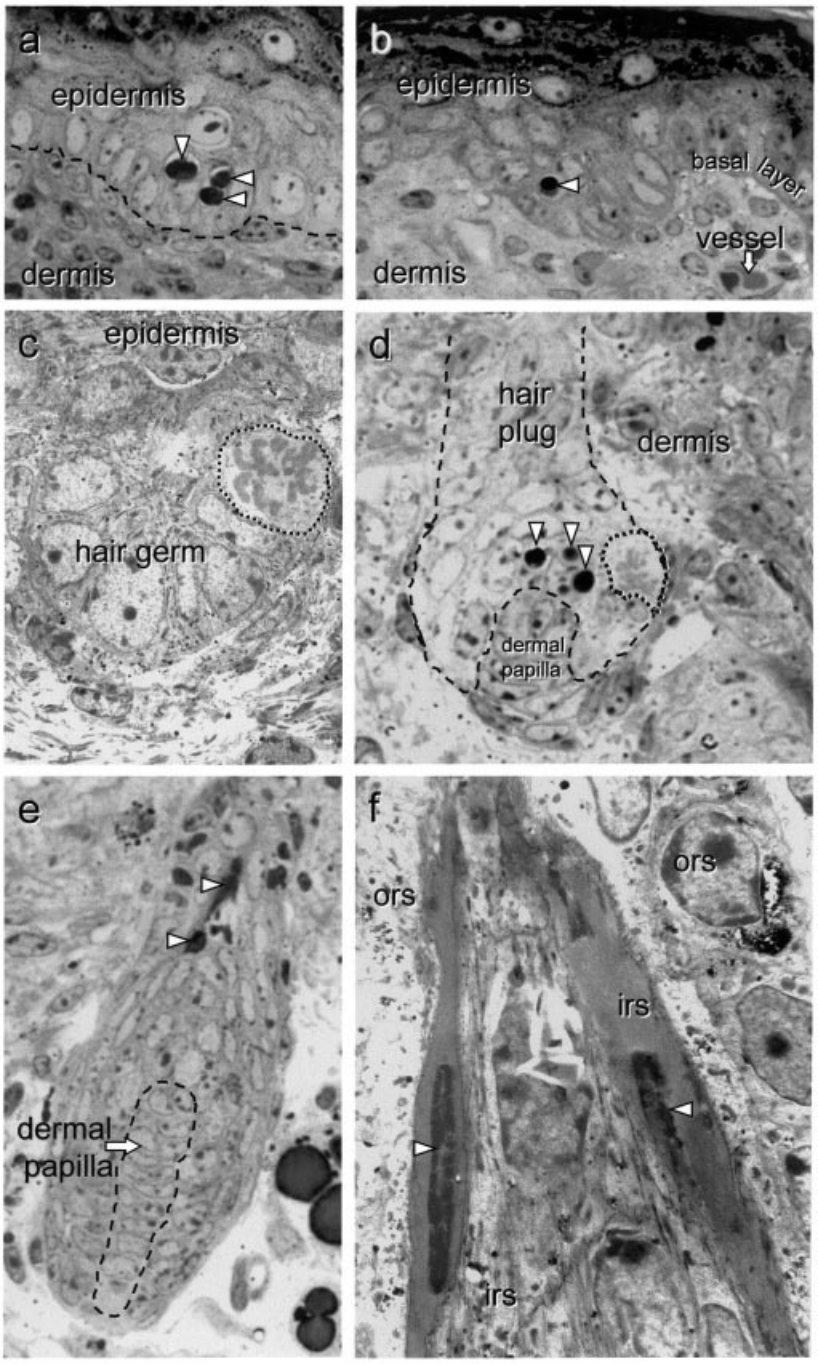

Figure 4. For the legend to this figure please see page 951.

Expression of ICE (caspase 1) during HF morphogenesis The distribution pattern of TUNEL$^+$ cells was correlated with the expression of ICE (caspase 1), a key enzyme in the death execution machinery of most cells (Zhivotovsky *et al*, 1996; Porter *et al*, 1997; Allen *et al*, 1998). During HF regression (catagen) in adolescent mice, we had previously demonstrated that all TUNEL$^+$ cells are located in regions of the HF epithelium that are also strongly ICE$^+$ (Lindner *et al*, 1997). Whereas epidermal KC were ICE$^+$ throughout HF morphogenesis, all KC in the HF were positive only until the hair bud had developed (**Fig 1***k–n*). Thereafter, ICE IR disappeared from the proximal hair bulb during the formation of the IRS (**Fig 1***o*, ***p***), which itself became strongly ICE$^+$ during stage 6 (**Fig 1***q*). The bulge (**Fig 1***q*, ***r***), the infundibulum, and the mid to distal ORS were ICE$^+$ during stages 6–8 (**Fig 1***r–v*). DP or connective tissue sheath fibroblasts never displayed any ICE IR during HF morphogenesis. In stage 6, prominent ICE IR was observed in precursor sebocytes (**Fig 1***q*). There was a gradual reduction in ICE IR in the IRS during stages 7 and 8 (**Fig 1***s*). The very prominent ICE IR in the early stages of HF morphogenesis (**Fig 1***k–n*) and the gradual yet marked decline in ICE IR in most of the middle and proximal part of the developing HF epithelium (**Fig 1***o–s*) raises the possibility that this caspase also has enzymatic functions that are unrelated to apoptosis control.

Correlation of TUNEL staining and morphology for assessment of apoptosis during HF morphogenesis Morphologic evidence of apoptosis was obtained using

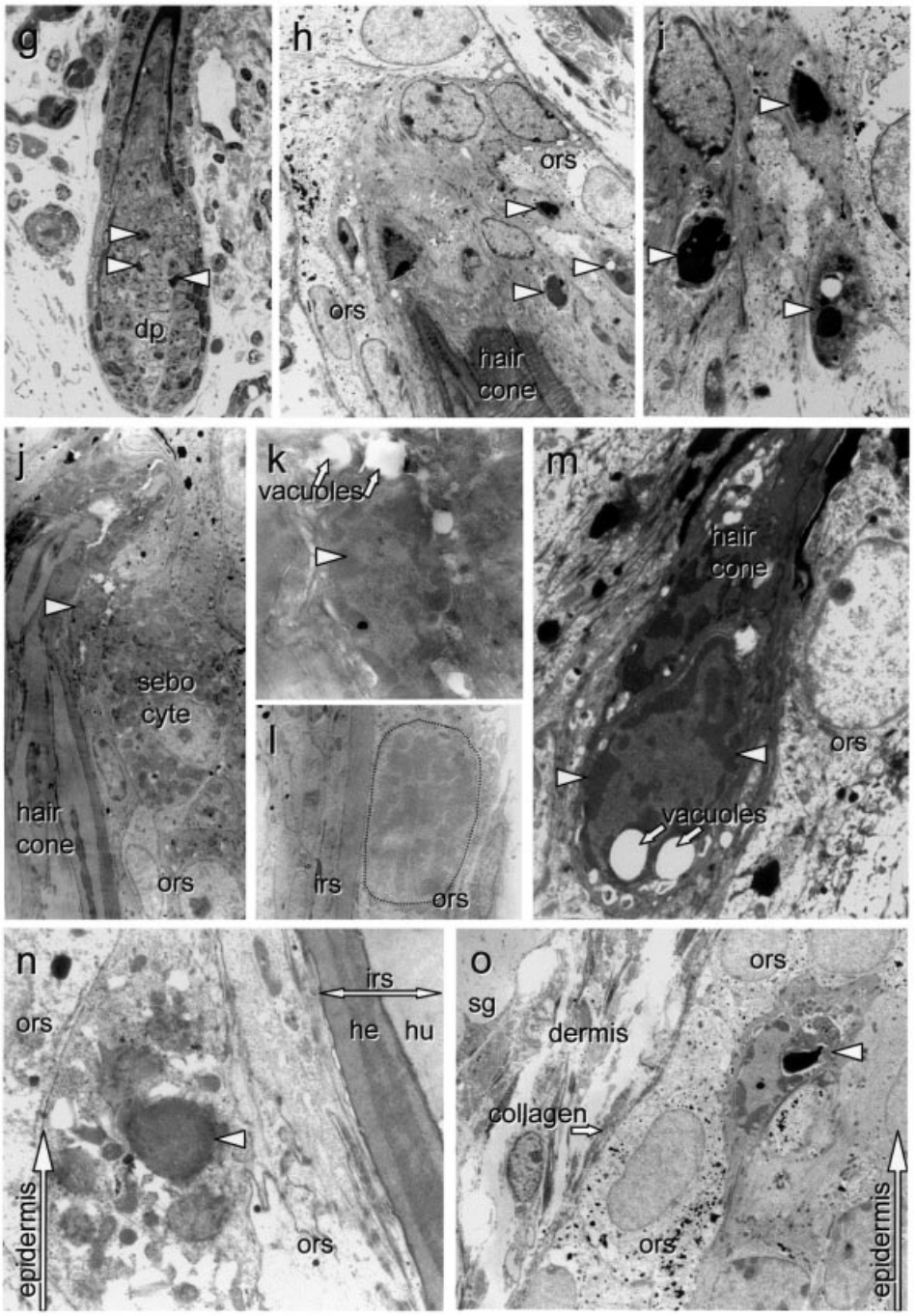

Figure 4. For the legend to this figure please see page 951.

HRLM for stages 1–8 HF in 0.5–1 μm resin sections, and was subsequently confirmed using transmission electron microscopy. Scattered apoptotic KC or clusters of apoptotic KC were detected in all follicular compartments throughout HF development (**Fig 4*a*–*k*, *m*–*o***), notably also during the earliest stages of HF development (**Fig 4*a*, *b*, *d***) when no TUNEL$^+$ cells were found.

Apoptosis was first convincingly detectable by HRLM/TEM during stages 1–2 (**Fig 4*a*, *b***). Here, scattered cells (**Fig 4*b***) or small clusters of two to four cells, invariably located in the suprabasal layer (**Fig 4*a***), were observed to contain portions of intensely staining cytoplasm, usually with a smooth contour and with small, densely basophilic (pyknotic) nuclei. There was considerable cell shrinkage associated with cytoplasmic contraction and loss of cell–cell junctions (leaving a halo around the cell). Interestingly, visible apoptosis occurred in the primitive hair germ (stage 2) (**Fig 4*b*, *c***), even before the formation of a recognizable DP. With advancing morphogenesis, stage 3–4 HF (**Fig 4*d*,** *dotted line*) exhibited clusters of apoptotic cells in the developing matrix just above the – now partially enclosed – DP. Cells undergoing apoptosis were observed in direct proximity to cells undergoing mitosis (**Fig 4*d***, *encircled area*). Yet, until stage 4 (**Fig 1*a*–*e*, *k*–*o***), no intrafollicular TUNEL$^+$ cells were found, whereas HRLM already revealed clusters of apoptotic KC in the HM just above the DP (**Fig 4*a*, *d*, *e***). Some intrafollicular TUNEL$^+$ KC displayed distinct morphologic features not typical for apoptotic cells, such as elongated nuclei and extended forms (**Fig 1*g*–*i*, *q*, *r***), instead of the shrunken and rounded phenotype (**Fig 1*i*, *l*, *r***) characteristic of TUNEL$^+$ apoptotic cells (Hossain *et al*, 1997; Trump *et al*, 1997). This suggests that these TUNEL$^+$ cells are terminally differentiating, rather than truly apoptotic KC.

Cell proliferation in the developing HF epithelium was common in stage 2–8 HF. When colocalized with apoptosis, proliferation tended to occur distally to these dying cells, particularly in the mid ORS or precortex region of the matrix. During stages 4–5 of HF morphogenesis, the developing IRS assumed a cone-shaped structure (**Fig 4*e*, *f***), consisting of terminally differentiating KC that were highly condensed and contained pyknotic nuclei. These cells, however, did not show classic apoptotic morphology. KC in the precortex region of the HM, however, exhibited classic apoptotic features including nuclear fragmentation and cytoplasmic condensation (**Fig 4*g***), whereas pyknotic IRS cells were highly extended in the hair growth direction and exhibited dissolution of cellular contents. Classic apoptosis was also regularly observed adjacent to the emerging hair cone during stages 6 and 7 (**Fig 4*h*–*k*, *m***). Apoptotic cells were also seen in other regions of the developing HF, including mid HF close to the IRS (**Fig 4*n***) and upper HF, at (**Fig 4*o***) and below (**Fig 4*h*, *i***) the level of the sebaceous gland. Ultrastructural analysis of these cells confirmed a diagnosis of apoptosis (Wyllie *et al*, 1981; Cotter *et al*, 1990). Consistent with the findings of Bullough and Laurence (1958) and our Ki67 data, mitotic cells were occasionally found in the middle ORS (**Fig 4*l***).

These differences between TUNEL staining and HRLM/TEM underscore the importance of using additional *in situ* techniques for apoptosis detection such as HRLM/TEM or confocal laser scanning microscopy (Cervos Navarro and Schubert, 1996; Kimura *et al*, 1997) in order to validate TUNEL data. Our findings demonstrate that TUNEL staining, at least in murine HF epithelium, is neither highly sensitive (false-negative results during earliest stages of HF development), nor highly specific (false-positive results during later HF morphogenesis).

In summary, methodologically, this study reports a novel triple staining for correlating apoptosis and proliferation in epithelial cell compartments and highlights that TUNEL data on HF apoptosis must be interpreted in conjunction with HRLM/TEM data to avoid false-negative and false-positive *in situ* end labeling results. Furthermore, this study further questions whether P-cadherin specifically discriminates proliferating from nonproliferating KC as suggested previously (Hirai *et al*, 1989; Shimoyama *et al*, 1989). Our study also reports the first profile of caspase 1 expression during HF development. This profile raises the possibility that this key death execution enzyme has functional properties in hair biology that extend beyond apoptosis. In addition, we show that developing murine HF are characterized by well-defined, developmentally controlled foci of proliferation and apoptosis. Finally, we present evidence that early HF development is not primarily a migratory phenomenon of epidermal invagination but a proliferation-driven event including apoptotic processes to control the effects of overproliferation and for fine sculpturing of the architecture of the follicle epithelium.

The excellent technical assistance of Ruth Pliet is most gratefully acknowledged. This study was supported in part by grants from the EU (Brite EURam Project No. BE 97-4301) to I.A.M. and R.P. and Deutsche Forschungsgemeinschaft to R.P. (Pa 345/8-2).

REFERENCES

Allen RT, Cluck MW, Agrawal DK: Mechanisms controlling cellular suicide: role of Bcl-2 and caspases. *Cellular Mol Life Sci May* 54:427–445, 1998

Ansari B, Coates PJ, Greenstein BD, Hall PA: *In situ* end-labelling detects DNA strand breaks in apoptosis and other physiological and pathological states. *J Pathol* 170:1–8, 1993

Bhat RV, DiRocco R, Marcy VR, et al: Increased expression of IL-1beta converting enzyme in hippocampus after ischemia: selective localization in microglia. *J Neurosci* 16:4146–4154, 1996

Botchkarev V, Botchkareva N, Albers K, van der Veen C, Lewin G, Paus R: Neutrophin-3 involvement in the regulation of hair follicle morphogenesis. *J Invest Dermatol* 111:279–285, 1998

Botchkarev V, Botchkareva N, Roth W, et al: Noggin is a mesenchymally derived stimulator of hair-follicle induction. *Nature Cell Biol* 3:158–164, 1999

Bullough WS, Laurence EB: The mitotic activity of the follicle. In: Montagna W, Ellis RA: eds. *The Biology of Hair Growth*. New York: Academic Press, 1958

Cervos Navarro J, Schubert TE: Pitfalls in the evaluation of apoptosis using TUNEL. *Brain Pathol* 6:347–348, 1996

Cotter TG, Lennon SV, Glynn JG, Martin SJ: Cell death via apoptosis and its relationship to growth, development and differentiation of both tumour and normal cells. *Anticancer Res* 10:1153–1159, 1990

Crissman HA, Steinkamp JA: Cell cycle-related changes in chromatin structure detected by flow cytometry using multiple DNA fluorochromes. *Eur J Histochem* 37:129–138, 1993

Danneel R: Die Entwicklung der Haare bei der Ratte. *Z Morph Ökol Tiere* 20:733–754, 1931

Darmon AJ, Bleackley RC: An interleukin-1beta converting enzyme-like protease is a key component of Fas-mediated apoptosis. *J Biol Chem* 271:21699–21702, 1996

Fleischhauer K: Über die Entstehung der Haaranordnung und das Zustandekommen räumlicher Beziehungen zwischen Haaren und Schweissdrüsen. *Z Zellforsch U Mikroskop Anat* 38:328–355, 1953

Fujita M, Furukawa F, Fujii K, Horiguchi Y, Takeichi M, Imamura S: Expression of cadherin cell adhesion molecules during human skin development: morphogenesis of epidermis, hair follicles and eccrine sweat ducts. *Arch Dermatol Res* 284:159–166, 1992

Gat U, DasGupta R, Degenstein L, Fuchs E: *De novo* hair follicle morphogenesis and hair tumors in mice expressing a truncated beta-catenin in skin. *Cell* 95:605–614, 1998

Gerdes J, Li L, Schlueter C, et al: Immunobiochemical and molecular biologic characterization of the cell proliferation-associated nuclear antigen that is defined by monoclonal antibody Ki-67. *Am J Pathol* 138:867–873, 1991

Gerlach C, Golding M, Larue L, Alison MR, Gerdes J: Ki-67 immunoexpression is a robust marker of proliferative cells in the rat. *Lab Invest* 77:697–698, 1997

Glücksmann A: Cell deaths in normal vertebrate ontogeny. *Biol-Rev* 26:59, 1951

Haake AR, Cooklis M: Incomplete differentiation of fetal keratinocytes in the skin equivalent leads to the default pathway of apoptosis. *Exp Cell Res* 231:83–95, 1997

Hardin JA, Sherr DH, DeMaria M, Lopez PA: A simple fluorescence method for surface antigen phenotyping of lymphocytes undergoing DNA fragmentation. *J Immunol Meth* 154:99–107, 1992

Hardy MH: The secret life of the hair follicle. *Trends Genet* 8:55–61, 1992

Hirai Y, Nose A, Kobayashi S, Takeichi M: Expression and role of E- and P-cadherin adhesion molecules in embryonic histogenesis. II. Skin morphogenesis. *Development* 105:271–277, 1989

Hossain MM, Nakayama H, Takashima A, Goto N, Doi K: 5-Azacytidine (5Az) induces apoptosis in PC12 cells: a model for 5Az-induced apoptosis in developing neuronal cells. *Histol Histopathol* 12:439–445, 1997

Karnovsky M: Formaldehyde-glutaraldehyde fixative of high osmolarity for use in electron microscopy. *Histopathol* 27:137–138, 1965

Kimura K, Sasano H, Shimosegawa T, et al: Ultrastructural and confocal laser scanning microscopic examination of TUNEL-positive cells. *J Pathol* 181:235–242, 1997

Lindner G, Botchkarev VA, Botchkareva NV, Ling G, van der Veen C, Paus R:

Analysis of apoptosis during hair follicle regression (catagen). *Am J Pathol* 151:1601–1617, 1997

Müller M, Jasmin JR, Monteil RA, Loubiere R: Embryology of the hair follicle. *Early Hum Dev* 26:159–166, 1991

Müller-Röver S, Peters EJM, Botchkarev VA, Panteleyev A, Paus R: Distinct patterns of NCAM expression are associated with defined stages of murine hair follicle morphogenesis and regression. *J Histochem Cytochem* 46:1401–1410, 1998

Müller-Röver S, Tokura Y, Welker P, Furukawa F, Wakita H, Takigawa M, Paus R: E- and P-cadherin expression during murine hair follicle morphogenesis and cycling. *Exp Dermatol* 4:237–246, 1999

Nose A, Takeichi M: A novel cadherin cell adhesion molecule: its expression patterns associated with implantation and organogenesis of mouse embryos. *J Cell Biol* 103:2649–2658, 1986

Oro AE, Scott MP: Splitting hairs: dissecting roles of signaling systems in epidermal development. *Cell* 95:575–578, 1998

Paus R, Rosenbach T, Haas N, Czarnetzki BM: Patterns of cell death: the significance of apoptosis for dermatology. *Exp Dermatol* 2:3–11, 1993

Paus R, Müller-Röver S, van der Veen C, et al: A comprehensive guide for the recognition and classification of distinct stages of hair follicle morphogenesis. *J Invest Dermat* 113:523–532, 1999

Philpott M, Paus R: Principles of hair follicle morphogenesis. In: Chuong CM (ed.): *Molecuar Basis of Epithelial Appendage Morphogenesis*. Austin, TX: Landes Bioscience Publication, 1998, pp. 75–103

Pinkus H: Embryology of hair. In: Montagna W, Ellis RA: eds. *The Biology of the Hair Growth*. New York: Academic Press, 1958

Polakowska RR, Piacentini M, Bartlett R, Goldsmith LA, Haake AR: Apoptosis in human skin development: morphogenesis, periderm, and stem cells. *Dev Dyn* 199:176–188, 1994

Porter AG, Ng P, Janicke RU: Death substrates come alive. *Bioessays* 19:501–507, 1997

Ramirez RD, Wright WE, Shay JW, Taylor RS: Telomerase activity concentrates in the mitotically active segments of human hair follicles. *J Invest Dermatol* 108:113–117, 1997

Sailer BL, Nastasi AJ, Valdez JG, Steinkamp JA, Crissman HA: Differential effects of deuterium oxide on the fluorescence lifetimes and intensities of dyes with different modes of binding to DNA. *J Histochem Cytochem* 45:165–175, 1997

Saunders JW Jr: Death in embryonic systems. *Science* 154:604–612, 1966

Sawhney N, Hall PA: Ki67-structure, function, and new antibodies. *J Pathol* 168:161–162, 1992

Schwarting R: Little missed markers and Ki-67. *Lab Invest* 68:597–599, 1993

Shimizu S, Eguchi Y, Kamiike W, Matsuda H, Tsujimoto Y: Bcl-2 expression prevents activation of the ICE protease cascade. *Oncogene* 12:2251–2257, 1996

Shimoyama Y, Hirohashi S, Hirano S, Noguchi M, Shimosato Y, Takeichi M, Abe O: Cadherin cell-adhesion molecules in human epithelial tissues and carcinomas. *Cancer Res* 49:2128–2133, 1989

St Jacques B, Dassule HR, Karavanova I, et al: Sonic hedgehog signaling is essential for hair development. *Curr Biol* 8:1058–1068, 1998

Tobin DJ, Fenton DA, Kendall MD: Ultrastructural observations on the hair bulb melanocytes and melanosomes in acute alopecia areata. *J Invest Dermatol* 94:803–807, 1990

Tobin DJ, Fenton DA, Kendall MD: Cell degeneration in alopecia areata. An ultrastructural study. *Am J Dermatopathol* 13:248–256, 1991

Trump BF, Berezesky IK, Chang SH, Phelps PC: The pathways of cell death: oncosis, apoptosis, and necrosis. *Toxicol Pathol* 25:82–88, 1997

Wyllie AH, Beattie GJ, Hargreaves AD: Chromatin changes in apoptosis. *Histochem J* 13:681–692, 1981

Zhivotovsky B, Burgess DH, Orrenius S: Proteases in apoptosis. *Experientia* 52:968–978, 1996